Eur. J. Biochem. **269**, 969–976 (2002) © FEBS 2002

Kinetic study of *sn*-glycerol-1-phosphate dehydrogenase from the aerobic hyperthermophilic archaeon, *Aeropyrum pernix* K1

Jin-Suk Han[1], Yoshitsugu Kosugi[2], Hiroyasu Ishida[2] and Kazuhiko Ishikawa[1]

[1]*National Institute of Advanced Industrial Science and Technology, Ikeda, Osaka, Japan;* [2]*National Institute of Advanced Industrial Science and Technology, Tsukuba, Ibaraki, Japan*

A gene having high sequence homology (45–49%) with the glycerol-1-phosphate dehydrogenase gene from *Methanobacterium thermoautotrophicum* was cloned from the aerobic hyperthermophilic archaeon *Aeropyrum pernix* K1 (JCM 9820). This gene expressed in *Escherichia coli* with the pET vector system consists of 1113 nucleotides with an ATG initiation codon and a TAG termination codon. The molecular mass of the purified enzyme was estimated to be 38 kDa by SDS/PAGE and 72.4 kDa by gel column chromatography, indicating presence as a dimer. The optimum reaction temperature of this enzyme was observed to be 94–96 °C at near neutral pH. This enzyme was subjected to two-substrate kinetic analysis. The enzyme showed substrate specificity for NAD(P)H-dependent dihydroxyacetone phosphate reduction and NAD^+-dependent glycerol-1-phosphate (Gro1*P*) oxidation. $NADP^+$-dependent Gro1*P* oxidation was not observed with this enzyme. For the production of Gro1*P* in *A. pernix* cells, NADPH is the preferred coenzyme rather than NADH. Gro1*P* acted as a noncompetitive inhibitor against dihydroxyacetone phosphate and NAD(P)H. However, $NAD(P)^+$ acted as a competitive inhibitor against NAD(P)H and as a noncompetitive inhibitor against dihydroxyacetone phosphate. This kinetic data indicates that the catalytic reaction by glycerol-1-phosphate dehydrogenase from *A. pernix* follows a ordered bi–bi mechanism.

Keywords: *Aeropyrum pernix*; archaea; glycerol-1-phosphate dehydrogenase; ordered bi–bi mechanism; hyperthermophile.

Archaea are a phylogenetically distinct group that diverged from eubacteria and eukaryotes at an early stage in evolution [1,2]. Archaea have several distinct features from eubacteria and eukaryotes, including the unique stereochemical backbones of phospholipids in their cellular membrane. The core lipid of the phospholipids and glycolipids in archaeal cells is *sn*-2,3-di-acylglycerol, which has a polar head group in the *sn*-1 position. In contrast, the major lipids of eukaryotic and bacterial cells mostly contain *sn*-1,2-di-acylglycerol, which has a polar head group in the *sn*-C-3 position [3]. Glycerol-1-phosphate (Gro1*P*) is the best substrate for the enzymatic synthesis of 2,3-digeranylgeranyl-*sn*-glcerol-1-phosphate in the moderate thermophilic (above 80 °C) *Methanobacterium thermoautotrophicum* [4]. Therefore, Gro1*P* dehydrogenase is identified as the key enzyme in the biosynthesis of archaeal enantiomeric polar lipid structures, such as the formation of Gro1*P* from CO_2 and the subsequent formation of the ether lipid from Gro1*P* in *M. thermoautotrophicum* [5,6]. The enzyme responsible for Gro1*P* formation of archaea-specific glycerophosphate, $NAD(P)^+$-dependent *sn*-glycerol-1-phosphate dehydrogenase, was initially found in *M. thermoautotrophicum* [7]. Although several properties were investigated, there has been no kinetic study of the mechanism of this enzyme. *Aeropyrum pernix* K1 (JCM number 9820) is the first aerobic hyperthermophilic archaea for which the complete genome sequence has been determined [8,9]. This archaeon's optimum growth temperature ranges from 90 to 105 °C. Most of the proteins from *A. pernix* are expected to be active at high temperature. The glycerol dehydrogenase gene in *A. pernix* K1 from the database provided by National Institute of Technology and Evaluation shows high similarity with the genes of some archaeal Gro1*P* dehydrogenases. To examine the function of the enzyme, we have cloned and expressed Gro1*P* dehydrogenase from *A. pernix* using *Escherichia coli*.

Correspondence to K. Ishikawa, The Special Division for Human Life Technology, National Institute of Advanced Industrial Science and Technology (Kansai), 1-18-31, Midorigaoka, Ikeda, Osaka 563-8577, Japan. Fax: + 81 727 51 9628, Tel.: + 81 727 51 9526, E-mail: kazu-ishikawa@aist.go.jp

Abbreviations: Gro1*P*, *sn*-glycerol-1-phosphate; Gro3*P*, *sn*-glycerol-3-phosphate, Gro, glycerol.

Enzymes: glycerol-3-phosphate dehydrogenase (NAD) (EC 1.1.1.8); glycerol dehydrogenase [NAD(P)] (EC 1.1.1.172); glycerol-1-phosphate dehydrogenase [NAD(P)] (EC 1.1.1.261).

(Received 5 October 2001, revised 5 December 2001, accepted 7 December 2001)

MATERIALS AND METHODS

Strain and culture condition

A. pernix K1 (JCM number 9820) was obtained from the Japan Collection of Microorganisms (Wako-shi, Japan). The culture media contained 37.4 g of Bacto marine broth 2216 (Difco) and 1.0 g of $Na_2S_2O_3{\cdot}H_2O$ in 1 L. The solution of $Na_2S_2O_3{\cdot}H_2O$ was separately sterilized by filtration, and aseptically added to the medium. *A. pernix* was cultivated for 48 h at 90 °C with shaking [8]. Genomic DNA was isolated from the cultivated cell of *A. pernix* by the method of Meade *et al.* [10].

Cloning and expression of the gene

Putative glycerol dehydrogenase gene (APE0519) from *A. pernix* was cloned by the method of Ishikawa *et al.* [11]. The gene was amplified using PCR with two primers containing unique restriction site. The upper primer (5′-CGTAACTAAGACTCCGGCATATGCTGTACCA TAGCGT-3′) contained an *Nde*I site as underlined. The lower primer (5′-AGGGGAAGAGAGGCAGGATCCCT AGC CAGACTATATA-3′) contained a *Bam*HI site as underlined. PCR amplifications were performed at 94 °C for 1 min, 61 °C for 2 min, and 70 °C for 3 min, for 35 cycles using Vent DNA polymerase. The amplified gene was hydrolyzed by the restriction enzymes and ligated to the pET11a (Novagen, Madison, USA). The inserted gene was transformed using pET11a vector system in the host *E. coli* BL21 (DE3) according to the manufacture's instructions (Novagen, Madison. USA), followed by sequence determination. Expression of the protein was induced by isopropyl thio-β-D-galactoside induction according to a previously reported method [11]. To verify the identity with the APE0519 sequence, DNA sequencing was carried out with a LI-COR Model LIC-4200(s)-2 Sequencer (Aloka, Mitaka, Tokyo, Japan). The concentration of the protein was determined with Coomassie protein assay reagent (Pierce Chemical Company, Rockford, IL, USA) using bovine serum albumin as the standard.

Purification of the Gro1*P* dehydrogenase from *E. coli*

The transformant cells were harvested by centrifugation and frozen at −20 °C. The cells were disrupted with aluminium oxide in 50 mM Tris/HCl buffer (pH 8.0). After incubation with DNase I (bovine pancreas, Sigma) for 30 min at 37 °C, the crude extract was heated at 85 °C for 30 min and centrifuged. The supernatant was dialyzed against 50 mM Tris/HCl buffer (pH 8.0) and the dialyzed sample was purified by chromatography using a HiTrap Q column (Pharmacia, Uppsala, Sweden), a HiLoad Phenyl Sepharose column (Pharmacia), and a HiLoad Superdex column (Pharmacia) according to the method described previously [12]. Multiple alignment of amino-acid sequences was done using the CLUSTAL W provided at http://www.ddbj.nig.ac.jp. The molecular mass of purified enzyme was determined by SDS/PAGE electrophoresis using 10–15% gradient gel of the Phast system (Pharmacia) and gel chromatography using HiLoad Superdex column. The N-terminal amino-acid sequence was analyzed using HP G1005 Protein Sequencing System at the Takara Shuzo Customer Service Center (Kusatsu, Japan).

Assay of Gro1*P* dehydrogenase activity

The activity of Gro1*P* dehydrogenase was determined in both directions, reduction and oxidation, spectrophotometrically at 340 nm as described by Nishihara & Koga [7]. The assay contained 50 mM Tris/HCl buffer (pH 7.0), 70 mM KCl, 2.1 mM dihydroxyacetone phosphate, and 0.32 mM NADH (0.32 mM NADPH) for the dihydroxyacetone phosphate reduction. The assay mixture for the Gro1*P* oxidation direction contained 50 mM Tris/HCl buffer (pH 7.0), 70 mM KCl, 10 mM Gro1*P*, and 5.0 mM NAD^+ (5.0 mM $NADP^+$). The reaction was performed at 65 °C in 1.5 mL cuvettes containing 1.2 mL reaction mixture and initiated by the addition of 10 μL of enzyme solution. Control reactions were carried out using the same reaction mixture without enzyme. The kinetic constants of Gro1*P* dehydrogenase of *A. pernix* were obtained from activity measurements, with substrate concentrations that ranged from $0.1 \times K_m$ to $10 \times K_m$. Each individual rate measurement was run in triple and the kinetic mechanism was determined by the damped nonlinear least-squares method (Marquardt–Levenberg method) [13,14].

Materials

Gro1*P* was prepared by dihydroxyacetone phosphate reduction using the purified enzyme solution [15]. The reaction mixture contained 4.2 mM dihydroxyacetone phosphate, 2.0 mM NADH, 50 mM Tris/HCl buffer (pH 7.0), and 50 μL purified enzyme solution. After the Gro1*P* formation reaction was completed at 65 °C for 6 h, Gro1*P* was purified by TLC chromatography [16] and its concentration was measured by the phosphate analysis [17]. Glyceraldehyde phosphate, dihydroxyacetone phosphate, *sn*-glycerol-2-phosphate, and dihydroxyacetone were purchased from Sigma. NADH, NAD^+, NADPH, and $NADP^+$ were used the products of the Oriental Yeast Co. Ltd.

RESULTS AND DISCUSSION

Alignment of amino-acid sequence of various dehydrogenases

The genome sequenced from *A. pernix* contained a putative glycerol dehydrogenase gene that consisted of a 1113 bp with an ATG initiation codon and a TAG termination codon. This gene encoded a 39 351-Da polypeptide consisting of 370 amino-acid residues. The deduced amino-acid sequence of Gro1*P* dehydrogenase was used for a similarity search in the protein resulting in strong similarity with those of Gro1*P* dehydrogenases from archaea. The results are summarized in Fig. 1. The sequence identity for *A. pernix* Gro1*P* dehydrogenase to the Gro1*P* dehydrogenase from *Methanobacterium thermoautotrophicum*, *Pyrococcus abyssi*, and *Sulfolobus solfataricus* was 45, 48, and 49%, respectively [6]. When compared to the glycerol (Gro) dehydrogenase from *E. coli, Schizosaccharomyces pombe*, and *Bacillus stearothermophilus*, the sequence identity was 19–20%. There was, however, no similarity with those $NAD(P)^+$-dependent *sn*-glycerol-3-phosphate (Gro3*P*) dehydrogenases which provided phospholipid backbones for bacteria. Many $NAD(P)^+$-dependent dehydrogenases have a similar folding pattern described as an 'ADP-binding βαβ fold' [18]. The NAD^+ binding sites of dehydrogenase have a highly conserved GXGXXG sequence, where X is any amino acid [19,20]. In contrast, some $NADP^+$ binding sites have an alanine at the position corresponding to the third glycine residue of the conserved trio [21]. In *A. pernix* Gro1*P* dehydrogenase, the NAD^+ binding site was found as conserved GXGXXG sequence at position 113–117. Some representative sequences of this conserved region are shown Fig. 2. Based on sequence alignment, the relative positions of the conserved sequences are the same in the Gro1*P* and

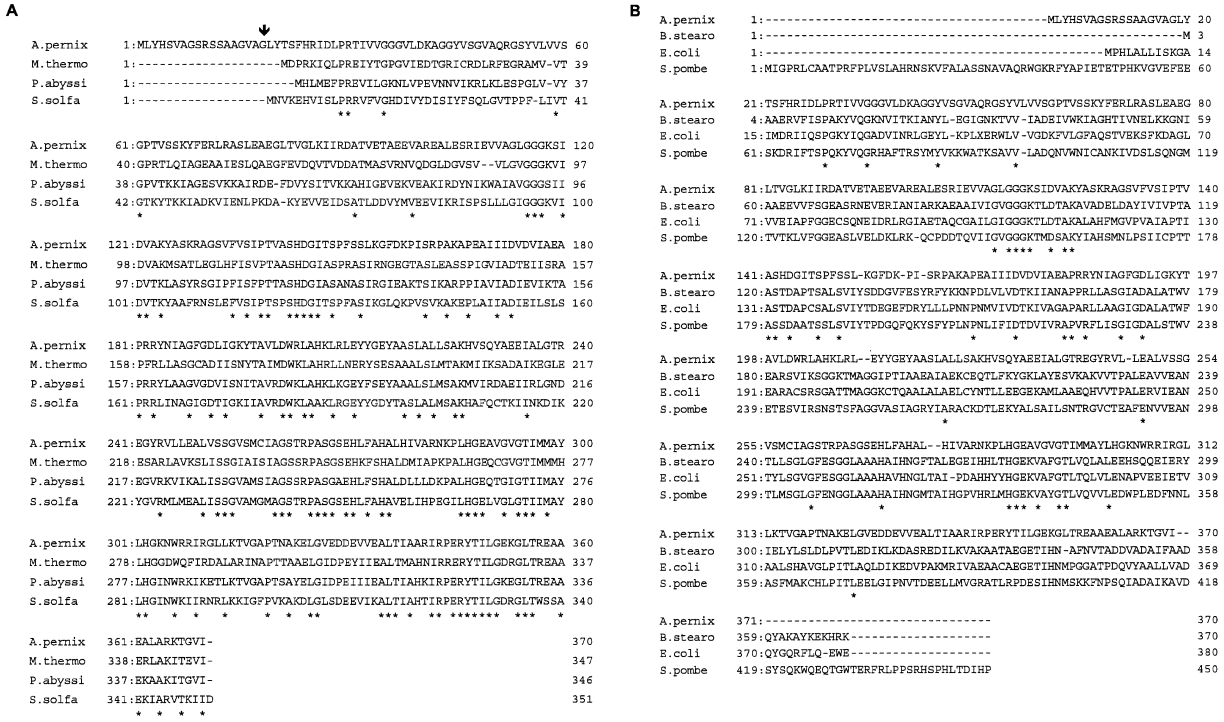

Fig. 1. Comparison of the amino-acid sequences of Gro1*P* dehydrogenase (A) and glycerol dehydrogenase (B). (A) Archaeal Gro1*P* dehydrogenase; M. thermo, *Methanobacterium thermoautotrophicum* (370 amino acids), P. abyssi, *Pyrococcus abyssi* (346 amino acids); S. solfa, *Sulfolobus solfataricus* (351 amino acids); (B) Glycerol dehydrogenase from bacteria and eukaryote; B. stero, *Bacillus stearothermophilus* (370 amino acids); E. coli, *Escherichia coli* (380 amino acids); S. pombe, *Schizosaccharomyces probe* (450 amino acids). The sequences have been aligned with dashes indicating gaps. Asterisks indicate conserved residues among four enzymes and an arrow indicates that the start point of amino acids in the purified enzyme.

Gro dehydrogenase families, suggesting a similar NAD^+-binding domain structure. On the other hand the relative positions of the conserved sequences differ dramatically between the Gro1*P* and Gro3*P* dehydrogenase families indicating a structural difference. Based on sequence homology, the gene product of APE0519 should be classified as a Gro1*P* dehydrogenase with a closer structural relationship to Gro dehydrogenases rather than Gro3*P* dehydrogenases [6].

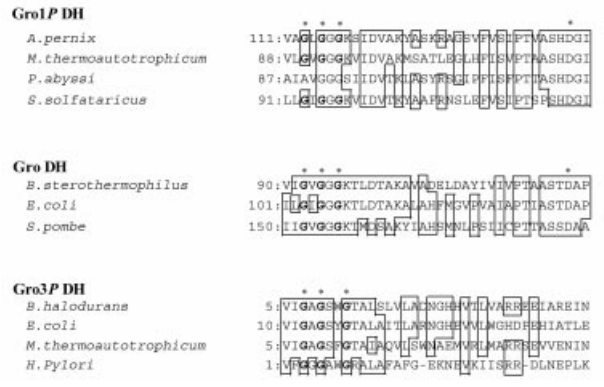

Fig. 2. Comparison of the amino-acid sequences of regions of representative $NAD(P)^+$-binding dehydrogenases. Conserved residues thought to be important for enzyme binding are marked with asterisks. The box indicates conserved residues between the enzymes. Gro1*P* DH, glycerol-1-phosphate dehydrogenase; Gro3*P* DH, glycerol-3-phosphate dehydrogenase; Gro DH, glycerol dehydrogenase.

Cloning of Gro1*P* dehydrogenase from *A. pernix*

The Gro1*P* dehydrogenase gene from *A. pernix* was amplified by PCR with unique two primers, inserted into pET11a, with the constructed plasmid transformed into BL21 (DE3). The sequence of the DNA inserted into the host cell was confirmed to have an identical sequence to the APE0519 gene. The Gro1*P* dehydrogenase of *A. pernix* was purified to homogeneity by a combination of ion exchange, hydrophobic, and gel chromatography. The purification procedure yielded approximately 4.4 mg of protein at a purification factor of about 147 with specific activity 3.22 $\mu mol \cdot min^{-1} \cdot mg^{-1}$ and recovery of 28% (Table 1). Sequencing of the purified protein in solution showed that the first seven N-terminal residues were Gly-Leu-Tyr-Thr-Ser-Phe-His. With the exception that 17 residues of N-terminal were deleted, the amino-acid sequence deduced was identical to that obtained in database. The sequence of the deleted segment does not seem to be a signal peptide [22]. The segment seems to be hydrolyzed during the process of purification. When tested as a dehydrogenase (dihydroxyacetone phosphate reduction), Gro1*P* dehydrogenase from *A. pernix* demonstrated NADH- and NADPH-dependent activity. The purified enzyme migrated as a single band on SDS/PAGE with apparent molecular mass of 38 kDa. The deduced amino-acid sequence of the open reading frame consisted of 367 amino acids with a molecular mass of 37 676 Da. The molecular mass estimated by gel chromatography (HiLoad Superdex) was approximately 72.4 kDa. This indicates that Gro1*P* dehydrogenase from *A. pernix* forms a dimer as

Table 1. Purification table of Gro1*P* dehydrogenase from *A. pernix*. The activity was measured in the direction of dihydroxyacetone phosphate reduction with the standard assay mixture.

Purification step	Total activity (units)	Protein (mg)	Specific activity ($\mu mol \cdot min^{-1} \cdot mg^{-1}$)	Yield (%)	Purification factor
Cell extract	51.46	2287	0.023	100	1
Heat treatment	44.99	113.9	0.40	87	17.6
HiTrap-Q	23.89	36.66	0.65	46	29.1
HiLoad Phenyl Sepharose	19.67	15.77	1.26	38	55.8
HiLoad Superdex	14.28	4.434	3.22	28	147.2

opposed to that from *M. thermoautotrophicum*, which exists as a homooctamer [7].

Substrate specificity and enzyme activity

The substrate specificity of Gro1*P* dehydrogenase was examined using the purified enzyme. No activity was observed toward glyceraldehyde phosphate, Gro3*P*, glycerol-2-phosphate (Gro2*P*), Gro, and dihydroxyacetone. This enzyme efficiently catalyzed the NADH- and NADPH-dependent dihydroxyacetone phosphate reduction, and also the NAD^+-dependent Gro1*P* oxidation (Table 2). The oxidation rate of $NADP^+$-dependent Gro1*P* was not detected, indicating that the enzyme has no or very low $NADP^+$-dependent Gro1*P* oxidation activity. The K_m value for dihydroxyacetone phosphate was 19.4-fold less than for Gro1*P* using NAD(H) as a coenzyme. This result suggests that the formation of Gro1*P* is the natural direction in the cell. The k_{cat} of the dihydroxyacetone phosphate reduction with NADH was higher than that with NADPH. The coenzyme NAD^+ was only used for the production of dihydroxyacetone phosphate. The Gro1*P* dehydrogenase from *A. pernix* showed NAD(P)H-dependent dihydroxyacetone phosphate reduction and NAD^+-dependent Gro1*P* oxidation activities. In contrast, Gro1*P* dehydrogenase from *M. thermoautotrophicum* was able to use both the NAD(H) and NADP(H) coenzymes for its oxidation/reduction reactions [7].

General properties of Gro1*P* dehydrogenase from *A. pernix*

Maximal activity of Gro1*P* dehydrogenase was seen between 94 and 96 °C at pH 7.0 (Fig. 3), which is in the normal temperature range for growth of *A. pernix* [8]. Over 96 °C, enzyme activity decreased dramatically, which seemed to be caused by irreversible denaturation of the enzyme. With the exception of the temperature-activity profile, the characteristics of the enzyme were determined from initial velocity measurements in the direction of the NADH-dependent dihydroxyacetone phosphate reduction at 65 °C chosen as dihydroxyacetone phosphate and NADH were rapidly decomposed over 70 °C [7]. The high growth temperature of *A. pernix* may be linked to the higher optimum activity temperature of its Gro1*P* dehydrogenase [24]. The half-life of activity was 30 min at the maximal activity temperature (95 °C) and increased to 2 h at 90 °C (Fig. 4). The enzyme activity of Gro1*P* dehydrogenase form *M. thermoautotrophicum* appeared to depend on the presence of K^+ and Na^+ and showed maximum activity at 70 mM of K^+[7]. However, the purified enzyme from *A. pernix* exhibited the highest levels of activity when assayed in metal free buffer after dialysis. Activity was decreased to 86 and 80% by addition of 70 mM K^+ and Na^+, respectively. This result shows that the activity of Gro1*P* dehydrogenase from *A. pernix* is affected differently by the intracellular concentration of K^+ than *M. thermoautotrophicum*.

Kinetic analysis of Gro1*P* dehydrogenase

The above results show that thermophilic Gro1*P* dehydrogenase catalyzes the following reaction:

$$DHAP + NAD(P)H + H^+ \rightleftarrows \text{Glycerol-1-phosphate} + NAD(P)^+$$

Table 2. Substrate specificity of Gro1*P* dehydrogenase from *A. pernix*. These parameters were estimated using nonlinear least-squares method [23] from experiments in which a fixed concentration of substrate or coenzyme and an appropriate range of concentration of the other reactant were used. ND; not detected.

Substrate	K_m (mM)	k_{cat} (min^{-1})
Dihydroxyacetone phosphate reduction		
Dihydroxyacetone phosphate (0.32 mM NADH)	0.460 ± 0.127	154.25 ± 43.29
Dihydroxyacetone phosphate (0.32 mM NADPH)	0.290 ± 0.128	45.21 ± 12.82
NADH (4 mM dihydroxyacetone phosphate)	0.032 ± 0.005	143.96 ± 6.81
NADPH (4 mM dihydroxyacetone phosphate)	0.044 ± 0.022	43.29 ± 5.12
Gro1*P* oxidation		
Gro1*P* (5 mM NAD)	8.92 ± 0.64	5.31 ± 0.11
Gro1*P* (5 mM NADP)	ND	ND
NAD (50 mM Gro1*P*)	1.57 ± 0.44	5.65 ± 0.45
NADP (50 mM Gro1*P*)	ND	ND

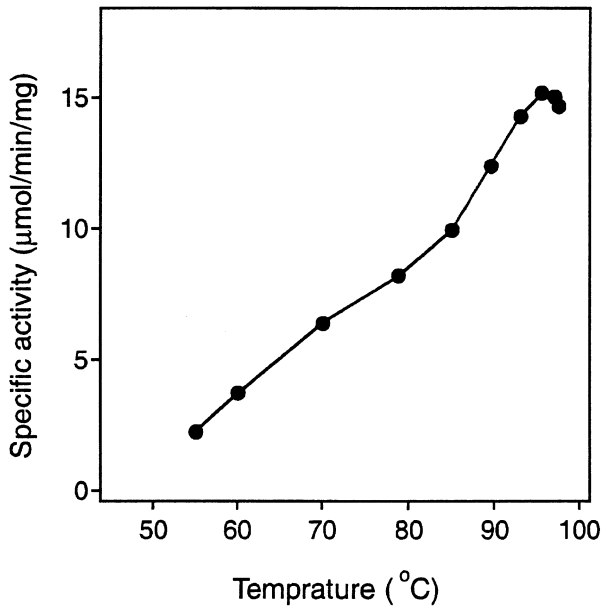

Fig. 3. Temperature dependence of specific activity for Gro1*P* dehydrogenase. The enzyme activity was measured in the direction of dihydroxyacetone phosphate reduction in 50 mM Tris/HCl buffer, pH 7.0, containing 70 mM KCl, 2.1 mM dihydroxyacetone phosphate, and 0.32 mM NADH for 5 min.

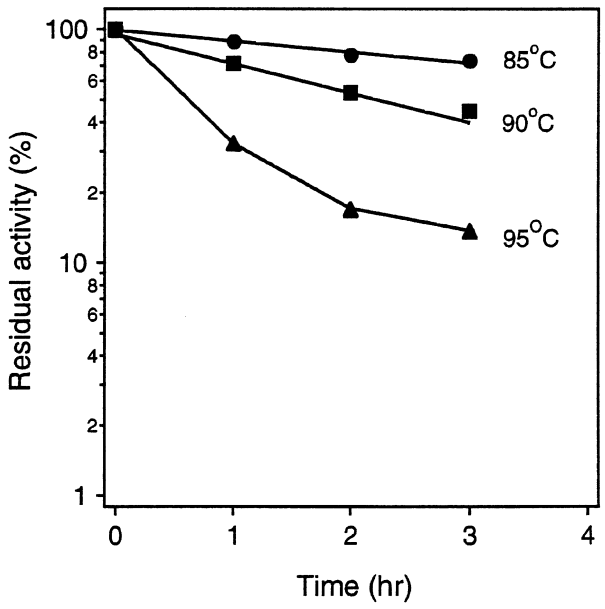

Fig. 4. Effect of heating on Gro1*P* dehydrogenase activity. Enzyme was incubated in 100 mM Tris/HCl buffer (pH 8.0). Aliquots were removed every hour and the activity was measured in the standard assay mixture at 65 °C. Residual activity is expressed on a logarithmic scale.

Initial velocities of the forward reaction were analyzed by varying the concentration of dihydroxyacetone phosphate and NAD(P)H under nonsaturating conditions without addition of reaction products. The reverse reaction using Gro1*P* and $NAD(P)^+$ could not be carried out because the backward rate was too low (see Table 2). The results of initial velocity studies were plotted on a Lineweaver–Burk (double reciprocal) plot (see A-1 and A-2 of Figs 5 and 6) [25]. The result of Figs 5 and 6 indicate that the saturation of the substrate was not reached under these conditions. Double reciprocal plots using dihydroxyacetone phosphate or NAD(P)H at various fixed levels of NAD(P)H or dihydroxyacetone phosphate, respectively, resulted in a family of lines with a common intersection to the left of the ordinate. This result excludes an 'equilibrium ordered bi–bi mechanism' and indicates a sequential mechanism [26]. To determine the binding order of substrates in a sequential mechanism, we carried out the product inhibition studies in which dihydroxyacetone phosphate or NAD(P)H was varied at nonsaturating levels. From the Lineweaver-Burk plots (see C-1 and C-2 of Figs 5 and 6), Gro1*P* acted as a noncompetitive inhibitor at various levels of NAD(P)H and dihydroxyacetone phosphate. Such an inhibition pattern ruled out a simple 'rapid equilibrium random bi–bi mechanism', a 'Theorell chance mechanism', or a 'ping-pong mechanism' [27]. The coproduct $NAD(P)^+$ [9] was found to be a noncompetitive inhibitor of the forward reaction when dihydroxyacetone phosphate was varied at the nonsaturated level of the coenzyme. However, it was not clear whether $NAD(P)^+$ acted as a competitive or noncompetitive inhibitor when NAD(P)H was varied at the nonsaturated level of dihydroxyacetone phosphate because the family of lines did not share a common intersection on the ordinate (see B-1 and B-2 of Figs 5 and 6). Within the range of experimental errors observed, this enzyme probably works using an 'ordered bi–bi mechanism'. Therefore, the experimental data was fitted to the equation for an 'ordered bi–bi mechanism' as follows [2].

$$V = \frac{\left(\frac{V_m[A][B]}{K_{ia}K_b}\right)}{\left(\left(1 + \frac{[A]}{K_{ia}} + \frac{K_a[B]}{K_{ia}K_b} + \frac{[A][B]}{K_{ia}K_b}\right) + \frac{K_q[P]}{K_pK_{iq}} + \frac{[Q]}{K_{iq}} + \frac{[P][Q]}{K_pK_{iq}} + \frac{K_q[A][P]}{K_{ia}K_pK_{iq}} + \frac{K_a[B][Q]}{K_{ia}K_bK_{iq}} + \frac{[A][B][P]}{K_{ia}K_bK_{ip}} + \frac{[B][P][Q]}{K_{ib}K_pK_{iq}}\right)}$$

where [A], [B], [P] and [Q] are the concentrations of NAD(P)H, dihydroxyacetone phosphate, Gro1*P*, and $NAD(P)^+$, respectively. The kinetics constants K_a (K_m for NAD(P)H), K_b (K_m for dihydroxyacetone phosphate), K_{ia} (dissociation constant for NAD(P)H), and V_m (maximal velocity) values were determined from the initial velocity studies ([P] = [Q] = 0) with a nonlinear least-squares method [14]. The K_{iq} (dissociation constant for $NAD(P)^+$) was obtained from the inhibition effect of $NAD(P)^+$ ([P] = 0). The K_{ip} (dissociation constant for Gro1*P*) and the K_p/K_q values were obtained from product inhibition studies of Gro1*P* (Q = 0). The K_p and K_q values are simultaneously present in the above equation as interdependent ratios. The experimental data was fitted to the above equation initial value of K_q set to 1. When the

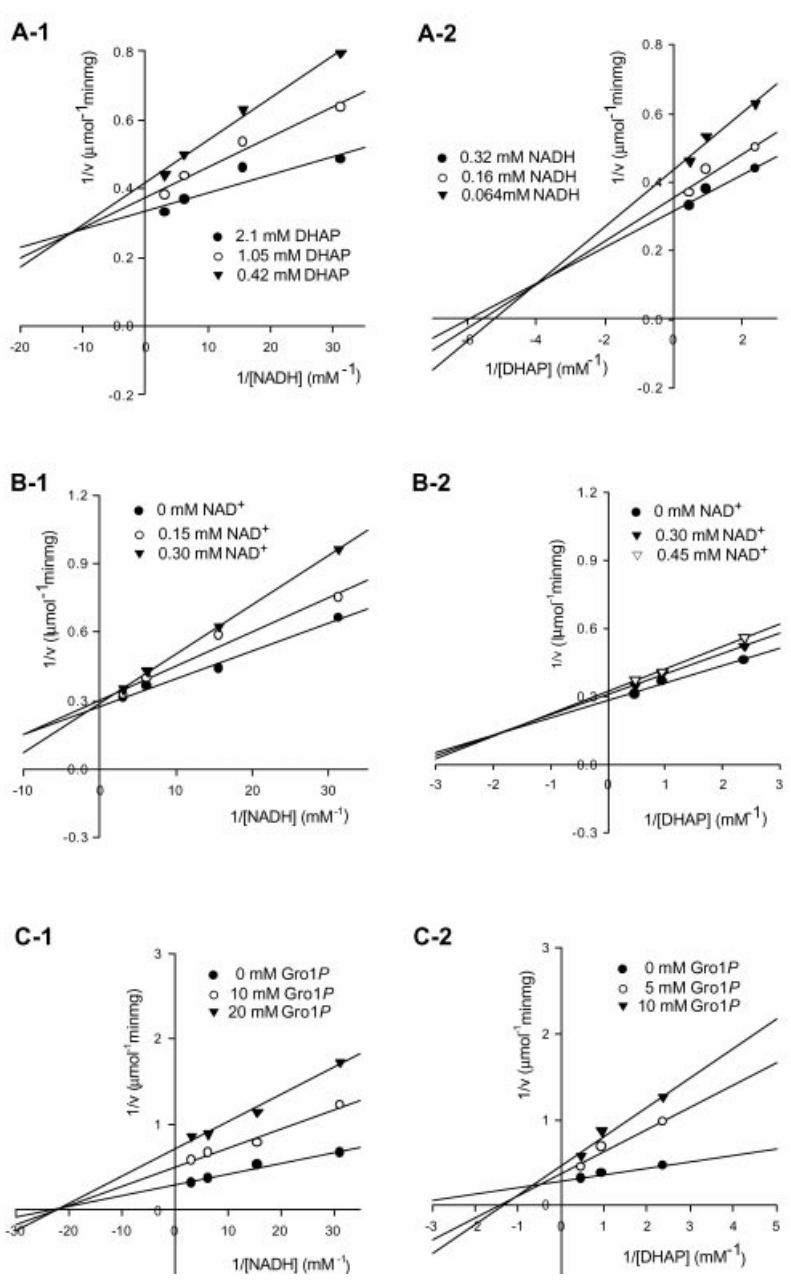

Fig. 5. Reciprocal plot of dihydroxyacetone phosphate (DHAP) reduction using NADH. A-1, initial velocity pattern with variable concentrations of NADH and nonsaturating fixed levels of dihydroxyacetone phosphate; A-2, initial velocity pattern with variable concentrations of dihydroxyacetone phosphate and nonsaturating fixed levels of NADH; B-1, inhibition of dihydroxyacetone phosphate reduction by NAD^+ at 2.1 mM dihydroxyacetone phosphate and varying NADH concentration; B-2, inhibition of dihydroxyacetone phosphate reduction by NAD^+ at 0.32 mM NADH and varying dihydroxyacetone phosphate concentration; C-1, inhibition of dihydroxyacetone phosphate reduction by Gro1*P* at 2.1 mM dihydroxyacetone phosphate and varying NADH concentration; C-2, Inhibition of dihydroxyacetone phosphate reduction by Gro1*P* at 0.32 mM NADH and varying dihydroxyacetone phosphate concentration. The enzyme activity was measured at 65 °C in 50 mM Tris/HCl buffer (pH 7.0) containing 70 mM KCl and variable concentration of substrates.

obtained values were plotted on a double reciprocal plot, $NAD(P)^+$ acted as a competitive inhibitor against NAD(P)H and a noncompetitive inhibitor against dihydroxyacetone phosphate, whereas Gro1*P* acted as a noncompetitive inhibitor against NAD(P)H and dihydroxyacetone phosphate. This supports the conclusion that this enzyme follows the ordered bi–bi mechanism. The final fitted values were 99.7% and 99.1% with final standard deviation of 0.016 and 0.010 using NADH and NADPH as coenzyme, respectively. The combination of results from initial velocity studies and inhibition patterns of products, suggest the reaction of Gro1*P* dehydrogenase is to be an 'ordered bi–bi mechanism'. Estimated kinetic parameters of the ordered bi–bi mechanism were summarized in Table 3. The K_b of NADPH (0.082 mM) was smaller than that of NADH (0.278 mM) indicating that NADPH is the better coenzyme for Gro1*P* production. The activity of this enzyme was regulated by the product, Gro1*P*, and $NAD(P)^+$ in contrast to the lack of product inhibition of the enzyme from *M. thermoautotrophicum* [7]. Although inhibition by Gro1*P* was relatively low such that K_{ip} against NADH was 31.47 mM and that against NADPH was 12.1 mM, the inhibitory effect could be confirmed by Figs 5 and 6 (C-1 and C-2). The observation that the $NADP^+$-dependent Gro1*P* oxidation activity was very low and the above kinetic results mean that Gro1*P* can efficiently control the reduction reaction without decreasing the Gro1*P* pool in the cell when NADPH is used as coenzyme. In contrast, the Gro1*P* dehydrogenase from *M. thermoautotrophicum* was not affected by Gro1*P* concentration during the production of Gro1*P* [7]. The inhibition mechanism in Gro1*P* dehydrogenase of *A. pernix* is different from that of

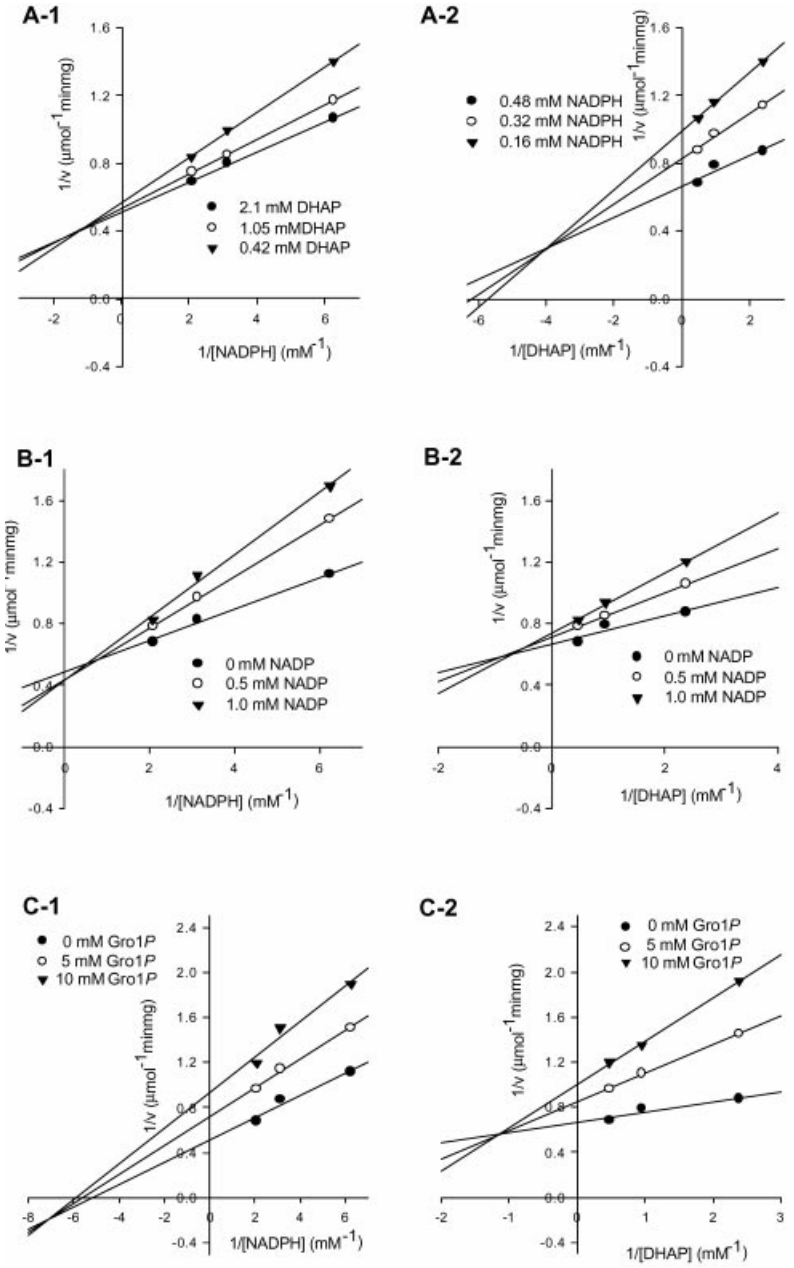

Fig. 6. Reciprocal plotting of dihydroxyacetone phosphate (DHAP) reduction using NADPH. A-1, initial velocity pattern with variable concentrations of NADPH and nonsaturating fixed levels of dihydroxyacetone phosphate; A-2, initial velocity pattern with variable concentrations of dihydroxyacetone phosphate and nonsaturating fixed levels of NADPH; B-1, inhibition of dihydroxyacetone phosphate reduction by $NADP^+$ at 2.1 mM dihydroxyacetone phosphate and varying NADPH concentration; B-2, Inhibition of dihydroxyacetone phosphate reduction by $NADP^+$ at 0.48 mM NADPH and varying dihydroxyacetone phosphate concentration; C-1, inhibition of dihydroxyacetone phosphate reduction by Gro1*P* at 2.1 mM dihydroxyacetone phosphate and varying NADPH concentration; C-2, inhibition of dihydroxyacetone phosphate reduction by Gro1*P* at 0.48 mM NADPH and varying dihydroxyacetone phosphate concentration. The enzyme activity was measured at 65 °C in 50 mM Tris/HCl buffer (pH 7.0) containing 70 mM KCl and variable concentration of substrates.

Table 3. Kinetic parameters for Gro1*P* dehydrogenase estimated by the ordered bi–bi function. These parameters were calculated from Figs 5 and 6 using the Marquardt-Levenbery method [13,14]. k_{cat} = turnover number, $K_a = K_m$ for NAD(P)H, $K_b = K_m$ for dihydroxyacetone phosphate, K_{ia} = dissociation constant for NAD(P)H, K_{iq} = dissociation constant for $NAD(P)^+$, K_{ip} = dissociation constant for Gro1*P*.

	Estimated value	
Kinetic parameter	NADH	NADPH
k_{cat} (min^{-1})	149.55 ± 12.06	73.47 ± 7.91
K_a (mM)	0.037 ± 0.014	0.159 ± 0.050
K_b (mM)	0.278 ± 0.099	0.082 ± 0.097
K_{ia} (mM)	0.020 ± 0.043	0.620 ± 0.245
K_{iq} (mM)	0.331 ± 0.028	1.03 ± 0.128
K_{ip} (mM)	31.5 ± 8.07	12.1 ± 2.74
K_p/K_q (—)	6.00 ± 0.49	2.68 ± 0.62
Final curve fitting (%)	99.7	99.1
Final SD of data (rms error)	0.016	0.010

M. thermoautotrophicum and also seems to be very important in the regulation of lipid biosynthesis. The Michaelis–Menten constant for Gro3*P* was over 50 mM in Gro3*P* dehydrogenase from *Saccharomyces cerevisiae*, so that the inhibitory effect of Gro3*P* was negligible in the experimental data. The Gro3*P* dehydrogenase in *E. coli* involved in lipid biosynthesis is regulated by allosteric inhibition by the production of Gro3*P*; this is important to maintain a low intracellular pool of Gro3*P* and to regulate lipid biosynthesis [28]. More detailed kinetic studies of Gro1*P* dehydrogenase should provide more information about how polar lipid biosynthesis in archaea differs from that in bacteria.

ACKNOWLEDGEMENTS

This work was performed as part of the STA fellowship program supported by the Japan Science and Technology Corporation.

REFERENCES

1. Nelson, K.H., Paulsen, I.T., Heidelberg, J.F. & Fraser, C.M. (2000) Status of genome projects for nonpathogenic bacteria and archaea. *Nat. Biotechnol.* **18**, 1049–1054.
2. Woese, C.R., Kandler, O. & Wheelis, M.L. (1990) Towards natural system of organisms: Proposal for the domains archaea, bacteria, and eucarya. *Proc. Natl Acad. Sci.* **87**, 4576–4579.
3. Zhang, D. & Poulter, C.D. (1993) Biosynthesis of archaebacterial ether lipids. Formation of ether linkages by prenyltransferases. *J. Am. Chem. Soc.* **115**, 1270–1277.
4. Zhang, D., Daniels, L. & Poulter, C.D. (1993) Biosynthesis of archaebacterial ether membranes. Formation of isoprene ethers by a prenyl transfer. *J. Am. Chem. Soc.* **115**, 1264–1265.
5. Nishihara, M. & Koga, Y. (1995) *sn*-glycerol-1-phosphate dehydrogenase in *Methanobacterium thermoautotrophicum*: key enzyme in biosynthesis of the enantiomeric glycerophosphate backbone of ether phospholipids of archaebacteria. *J. Biochem.* **117**, 933–935.
6. Koga, Y., Kyuragi, T. & Sone, N. (1998) Did archeal and bacterial cell arise independently from noncellular precursors? A hypothesis stating that advent of membrane phospholipid with enantiomeric glycerophosphate backbones caused the separation of the two lines of descent. *J. Mol. Evol.* **46**, 54–63.
7. Nishihara, M. & Koga, Y. (1997) Purification and properties of *sn*-glycerol-1-phosphate dehydrogenase from *Methanobacterium thermoautotrophicum*: Characterization of the biosynthetic enzyme for the enatiomeric glycerophosphate backbone of ether polar lipids of archaea. *J. Biochem.* **122**, 572–576.
8. Sako, Y., Nomura, N., Uchida, A., Ishida, Y., Morri, H., Koga, Y., Hoaki, T. & Maruyama, T. (1996) *Aeropyrum pernix* General Nov., sp. Nov., a novel aerobic hyperthermophilic archaeon growing at temperatures up to 100 °C. *Int. J. Syst. Bacteriol.* **46**, 1070–1077.
9. Faguy, D.M. & Doolittle, W.F. (1999) Genomics: lessons from the *Aeropyrum pernix* genome. *Current Biol.* **9**, R883–R886.
10. Meade, H.M., Long, S.R., Ruvkun, G.B., Brown, S.E. & Ausubel, F.M. (1982) Physical and genetic characterization of symbiotic and auxotrophic mutants of *Rhizobium meliloti* induced by transposon Tn5 mutagenesis. *J. Bacterial.* **149**, 114–122.
11. Ishikawa, K., Ishida, H., Koyama, Y., Kawarabayasi, Y., Kawahara, J., Matsui, E. & Matsui, I. (1998) Acylamino acid-releasing enzyme from the thermophilic archaeon *Pyrococcus horikoshii*. *J. Biol. Chem.* **273**, 17726–17731.
12. Ishikawa, K., Ishida, H., Matsui, I., Kawarabayasi, Y. & Kikuchi, H. (2001) Novel bifunctional hyperthermostable carboxypeptidase/aminoacylase from *Pyrococcus horikoshii* OT3. *Appl. Environ. Microbiol.* **67**, 673–679.
13. Menke, W. (1989) Discrete inverse theory. In *Geophysical Data Analysis*, Revised edn, pp. 143–160. Academic Press, New York, USA.
14. Press, W.H., Teukolsky, S.A., Vertterling, W.T. & Flannery, B.P. (1992) *Numerical Recipes in Fortran – the Art of Scientific Computing*, 2nd edn. Cambridge University Press, USA.
15. Nishihara, M., Yamazaki, T., Oshima, T. & Koga, Y. (1999) *sn*-Glycerol-1-phosphate-forming activities in Archaea: Separation of archaeal phospholipid biosynthesis and glycerol catabolism by glycerophosphate enantiomers. *J. Bacteriol.* **181**, 1330–1333.
16. Nishihara, M. & Koga, Y. (1988) Quantitative conversion of diether and tetraether phospholipids to glycerophosphoesters by dealkylation with boron trichloride: a tool for structural analysis of archaebacterial lipids. *J. Lipid Res.* **29**, 384–388.
17. Bartlett, G.R. (1959) Colorimetric assay methods for free and phosphorylated glyceric acids. *J. Biol. Chem.* **234**, 469–471.
18. Fan, F. & Plapp, B.V. (1999) Probing the affinity and specificity of yeast alcohol dehydrogenase I for coenzymes. *Arch. Biochem. Biophys.* **367**, 240–249.
19. Wierenga, R.K., Terpsta, P. & Hol, G.J. (1986) Prediction of the occurrence of the ADP-binding βαβ-fold in proteins, using an amino acid sequence fingerprint. *J. Mol. Biol.* **187**, 101–107.
20. Nagy, E., Henics, T., Eckert, M., Lightowlers, R.N., Kellermayer, M. & Miseta, A. (2000) Identification of the NAD^+-binding fold of glyceraldehyde-3-phosphate dehydrogenase as a novel RNA-binding domain. *Biochem. Biophys. Res. Commun.* **275**, 253–260.
21. Scrutton, N.S., Berry, A. & Perham, R.N. (1990) Redesign of the coenzyme specificity of a dehydrogenase by protein engineering. *Nature* **343**, 38–43.
22. Marion, E.E.W. (1984) Complication of published signal sequences. *Nucleic Acids Res.* **12**, 5145–5164.
23. Sakoda, M. & Hiromi, K. (1976) Determination of the best-fit values of kinetic parameters of the Michaelis–Menten equation by the method of the least squares with the Taylor expansion. *J. Biochem. (Tokyo)* **80**, 547–555.
24. Yamano, S., Sako, Y., Momura, N. & Maruyama, T. (1999) A cambialistic SOD in a strictly aerobic hyperthermophilic archaeon, *Aeropyrum pernix*. *J. Biochem.* **126**, 218–225.
25. Rudolph, F.B. & Fromm, H.J. (1979) Plotting methods for analyzing enzyme rate data. In *Methods in Enzymology* (Purich, D.L., ed.), pp. 138–158. Academic Press, San Diego, CA.
26. Cleland, W.W. (1963b) The kinetics of enzyme-catalyzed reactions with two or more substrates or products. 2. Inhibition: nomenclature and theory. *Biochim. Biophys. Acta* **67**, 173–187.
27. Cai, J., Pietzsch, M., Theobald, U. & Rizzi, M. (1996) Fast purification and kinetics studies of the glycerol-3-phosphate dehydrogenase from the yeast *Saccharomyces cerevisiae*. *J. Biotechnol.* **49**, 19–27.
28. Edger, J.R. & Bell, R.M. (1978) Biosynthesis in *Escherichia coli* of *sn*-glycerol-3-phosphate, a precursor of phospholipid. Kinetic characterization of wild type and feed-back-resistant forms of the biosynthetic *sn*-glycerol-3-phosphate dehydrogenase. *J. Biol. Chem.* **253**, 6354–6363.